IC/93/246

INTERNATIONAL CENTRE FOR THEORETICAL PHYSICS

FRAGMENTATION OF $Ge_{1-x}\ Sn_x\ Se_2$ GLASSES

G. Saffarini

INTERNATIONAL ATOMIC ENERGY AGENCY

UNITED NATIONS EDUCATIONAL, SCIENTIFIC AND CULTURAL ORGANIZATION

MIRAMARE-TRIESTE

IC/93/246

International Atomic Energy Agency
and
United Nations Educational Scientific and Cultural Organization
INTERNATIONAL CENTRE FOR THEORETICAL PHYSICS

FRAGMENTATION OF $Ge_{1-x}\ Sn_x\ Se_2$ GLASSES

G. Saffarini [1]
International Centre for Theoretical Physics, Trieste, Italy.

ABSTRACT

Density, differential scanning calorimetry (DSC), X-ray diffraction (XRD), and X-ray photoelectron spectroscopy (XPS) measurements of $Ge_{1-x}Sn_xSe_2$ within $0.0 \leq x \leq 0.6$ have been obtained. Upon increasing the Sn content, the density measurements show a non-monotonic decrease, while the differential scanning calorimetry measurements show a monotonic decrease of the glass transition temperature. The X-ray diffraction measurements on these glasses give interference functions which have first sharp diffraction peaks (FSDP) indicating the presence of intermediate range order (IRO). The X-ray photoelectron spectroscopy measurements were used to determine the plasmon energies from the $L_3M_{4,5}M_{4,5}$ selenium Auger peaks which may be looked upon as being determined by the local electron density about the selenium atoms. It is found that the plasmon energies deduced from the Auger peaks change markedly with the Sn content in these glasses. These results are consistent with the fragmentation of the molecular cluster network model proposed by Mikrut and McNeil.

MIRAMARE–TRIESTE
August 1993

[1]Permanent address: Physics Department, An-Najah National University, Nablus, Via Israel.

1 Introduction

The structure of a-$GeSe_2$ has been widely studied in the past few years [2-11], but the debate about the model which best describes it, is still open. Two basic types of models have been proposed. The first model, the chemically–ordered covalent network (COCN) model, assumes that a-$GeSe_2$ consists of corner– and edge–sharing $Ge(Se_{1/2})_4$ tetrahedra linked together to form a three–dimensional network [3]. In this model, wrong homopolar bonds are minimized and appear only as defects. The second model, the outrigger raft (OR) model (also known as the molecular cluster network [MCN] model) was proposed by [7,12]. This model favours two–dimensional local atomic arrangements and assumes that a-$GeSe_2$ consists of modified fragments of the layer–crystal structure. The fragments are laterally bordered by $Se - Se$ edge dimers. Thus this model assumes that wrong homopolar bonds are an intrinsic property of the structure of a-$GeSe_2$.

The aim of this paper is two–fold. The first is to probe the structural changes introduced when Sn, in varying concentrations, is added to a-$GeSe_2$. The second is to lend support to one of the above mentioned models proposed for the structure of covalently bonded glasses. To achieve this, density, DSC, XRD, and XPS measurements have been performed on $Ge_{1-x}Sn_xSe_2$ glasses.

2 Experimental procedures

The glasses were prepared by the conventional melt quenching method using high purity elements (99.999%). The method consisted of sealing, at a pressure of approximately 10^{-5} Torr, the weighted amounts of the constituent elements in a carefully outgassed, argon flushed, rectangular–section silica ampoules ($1.5 \times 1.5 \times 6.0$ cm). The ampoules were then placed in a rocking furnace in which they were heated to a temperature of 1050°C and were agitated to ensure thorough mixing of the melt. After homogenizing for three days, the ampoules were quenched to room temperature in a large volume water bath.

The macroscopic densities at room temperature of the as–prepared glasses were measured by the Archimedes method using ethyl–methyl ketone ($C_2H_5 - CO - CH_3$) as the immersion liquid which has a density of $0.803 - 0.805$ gcm^{-3} at 20°C. The densities were calculated using the formula

$$\rho_g = (\omega_0/[\omega_0 - \omega_L])\,\rho_L$$

where ω_0 and ω_L represent the weight of the sample in air and in the liquid, respectively, and ρ_L is the density of the immersion liquid.

A Perkin–Elmer DSC–2C differential scanning calorimeter using a scan rate of 20K/min and sample sizes of 40 mg of the powdered glass, was utilised to study the glass transition temperatures. The powdered samples were sealed in aluminium pan and compared with an empty aluminium pan. The measurements were performed in dried, oxygen free, nitrogen atmosphere. The glass transition temperature, T_g, was taken at the midpoint of the step in the thermogram.

The flat surfaces of the as–quenched glasses adjacent to the walls of the silica tubes provided good surfaces for X–ray analysis. The X–ray diffraction measurements were performed on a $\theta - \theta$ X–ray diffractometer (after removal of the silica wall) using $Mo\ K_\alpha$ radiation ($\lambda = 0.71069$ Å). A distinguishing feature of these X–ray measurements is that only as–quenched virgin surfaces were examined.

The X-ray photoelectron spectroscopy measurements of the as-quenched surfaces were carried out in ES300 electron spectrometer using $Al\ K_\alpha$ X-rays as the exciting radiation.

3 Results

The density results (Fig.1) show that there is a non-monotonic decrease in density upon increasing the Sn concentration in these glasses. This behaviour of the density results will be discussed later.

The variation of the glass transition temperatures (T_g) with Sn content in these glasses is shown in Fig.2. The glass transition temperatures show a monotonic decrease upon increasing Sn content. The results of [1] are plotted for comparison. It is clear that our T_g values are larger than those reported by [1]. This difference may be attributed to the differing thermal history of the glasses, which greatly influences the final structure of the glass. Our higher T_g values (i.e. higher by 16 K for $GeSe_2$ as compared to those reported by [1]) may be taken as an indication that our glasses are more stable (i.e. possess lower configurational entropy and more heteropolar bonds).

The X-ray interference functions for $x = 0.1, 0.2, 0.3, 0.4$ and 0.5 are shown in Fig.3. They show a first sharp diffraction peak (FSDP). The peak fit parameters (position in reciprocal space, full width at half-maximum Δk [FWHM], coherence length [L], and the height ratio of the FSDP to the second peak) are given in Table 1. The coherence length, which is related via an approximate relation to the FWHM by the expression $L \sim (2\pi/\Delta k)$ [13], decreases from 39 Å for $GeSe_2$ to 17 Å for $Ge_{0.5}Sn_{0.5}Se_2$. This reduction of the coherence length is correlated with a decrease in the height ratio of the FSDP to the second peak of the interference functions indicating a reduction of the amount of intermediate range order (IRO).

The average values of plasmon energies deduced from the $L_3M_{4,5}M_{4,5}$ Auger lines of selenium are given in Table 2. Fig.4 shows the plasmon energy losses for the two compositions $Ge_{0.7}Sn_{0.3}Se_2$ and $Ge_{0.5}Sn_{0.5}Se_2$. The plasmon energies, calculated using the relation $\hbar\omega_p = \hbar(ne^2/\epsilon_0 m)^{1/2}$ [14, 15] where n is the valence electron density, are also given in Table 2. The change in plasmon energy with Sn content in the glasses, both for calculated values and those determined experimentally from the $L_3M_{4,5}M_{4,5}$ Auger lines of selenium, are shown in Fig.5. It can be seen from Table 2 and Fig.5 that the measured plasmon energy losses are always larger than the calculated values. The experimentally determined values of the plasmon energies were used to calculate the average energy gaps of the $Ge-Se$ bonds. The calculation was done by making use of a simple model, based on the plasma frequency formalism, developed by [16] for $A^{II}B^{IV}C_2^V$ semiconductors. In our calculation we assumed that the ternary additive Sn can take on the role of a group-II element and that Se takes on the role of a group-V element. The change in the calculated values of the average energy gaps and the measured optical energy gaps [17] with Sn content in the glasses are shown in Fig.6. In this figure, the values of the optical energy gaps were normalized to the value of the average energy gap of $GeSe_2$. It is interesting to note that the average energy gaps and the measured optical energy gaps [17] seem to reflect each other in spite of the difference in the way they have been obtained.

4 Discussion

The density results show that there is a decrease in density as Sn is added to $GeSe_2$ (Fig.1). This type of behaviour observed for the density, indicates that the glass network "raft" is progressively fragmenting with increasing Sn concentration. Moreover, between $x = 0.2$ and $x = 0.3$ there is a sudden drop in density, marking the onset of fragmentation at $x = 0.2$. Apparently as the "raft" breaks up the free interfacial volume between the fragments increases and the ratio of the surface to volume of the molecular clusters will increase, thus resulting in the decrease of the density. The observed monotonic decrease in the glass transition temperature with increasing Sn concentration (Fig.2) is consistent with that reported by [1] and does not show the step-like behaviour between $x = 0.4$ and $x = 0.5$ observed by [18]. This smooth monotonic decrease indicates that the glass is becoming less stable and that the configurational entropy is increasing, and is consistent with an increase in the ratio of the surface to volume of the molecular clusters which would occur as the "rafts" break up and their sizes decrease. A slight contribution to the decrease in the glass transition temperatures is attributable to the replacement of the stronger bond $Ge-Se$ (49.08 k cal/mole) by the weaker bond $Sn-Se$ (47.38 k cal/mole) [19].

Mikrut and McNeil [1] proposed a model for the structure of these ternary glasses, based on the model of a-$GeSe_2$ proposed by [7], in which Sn atoms substitute preferentially the Ge atoms situated on the edge of the cluster "outrigger raft". As Sn concentration is increased, the average-size cluster can no longer accommodate all of the Sn atoms substitutionally in the preferred Ge sites on the edge of the cluster "outrigger sites". The cluster, therefore break up into smaller clusters to create more "outrigger sites" for the Sn atoms to occupy. This fragmentation begins to occur at the value $x = 0.2$ and as x increases, Sn atoms continue to occupy "outrigger sites" until the clusters reduce to the smallest possible unit which retains the bonding of a-$GeSe_2$, namely one consisting of two chains. For $x > 0.7$ the structure of crystalline $SnSe_2$ begins to dominate and the sample can no longer form a glass. However, it was not possible to prepare a truly amorphous sample for $x > 0.6$ with the cooling technique employed in this work, in the sense that the X-ray diffraction pattern displays sharp peaks characteristic of crystallization. This was attributed to the slower cooling rates for our samples because of the larger sample sizes prepared. The density results reported here are consistent with this model proposed by [1].

The observed FSDP on the X-ray interference functions for the glassy compositions examined indicate the presence of (IRO) for these alloys and is in accord with the observation of the companion mode (A_1^C) in the Raman spectra obtained by [1] for all concentrations up to $x = 0.7$. This companion mode is generally associated with (IRO) of the glass network [7]. The decrease of the coherence length when Sn is added to a-$GeSe_2$ (see Table 1) indicates that the average size of the clusters associated with (IRO) is decreasing, which is consistent with the fragmentation into smaller clusters when Sn is added to a-$GeSe_2$.

It has been shown [20] that the measured plasmon energies deduced from the $L_3M_{4,5}M_{4,5}$ selenium Auger peaks serve as a local probe of the selenium electron density in chalcogenide glasses. Fig.5 shows that the local electron density of selenium atoms decreases when Sn is added to a-$GeSe_2$. It must be noted that this decrease of the local electron density results from a decrease of the amount of intermediate range order (IRO) that is

present in these glasses [21].

It has been suggested by [17] that the electrons beyond the mobility edge become localized in a smaller volume as the cluster size is decreased in the composition range $0.2 \leq x \leq 0.3$. This leads to an increase in the energy of the anti-bonding states and thus in optical band gap and average energy gap. The calculated average energy gaps from the measured plasmon energies from the $L_3M_{4,5}M_{4,5}$ Auger lines of selenium (Fig.6) show an increase at $x = 0.3$ from the otherwise decreasing trend which can be explained on this basis. Thus the behaviour of the average energy gap parallels that of the optical energy gap of [17].

Further information on the glass structure comes from the value of the average coordination number of the glasses examined which remains constant at $< m > = 2.67$ (see Table 2). *According to* [22] *this value of* $< m >$ *corresponds to a topological threshold and* is associated with two dimensional (2D) layered structures. Therefore, the idea proposed by [18] that there is a transition from molecular cluster network (MCN) to continuous random network (CRN) occurring at $x = 0.35$, is not supported.

5 Conclusion

The compositional dependence of the density and the decrease of the coherence length (when Sn is added to a-$GeSe_2$) serve as extra strong evidence in support of the fragmentation of the molecular cluster network model, proposed by [1], for the structure of $Ge_{1-x}Sn_xSe_2$ glasses.

Acknowledgments

The author would like to thank Professor Abdus Salam, the International Atomic Energy Agency and UNESCO for hospitality at the International Centre for Theoretical Physics, Trieste, where this work was completed. He also wishes to thank Professor Yu Lu, the leader of the Condensed Matter Physics Group (CMG) at ICTP, for reading the manuscript.

REFERENCES

[1] J.M. Mikrut and L.E. McNeil, J. Non-Cryst. Solids **109** (1989) 237.

[2] J.C. Malaurent and J. Dixmier, J. Non-Cryst. Solids **35** & **36** (1980) 1227.

[3] P. Tronc. M. Bensoussan, A. Brenac and C. Sebenne, Phys. Rev. **B8** (1973) 5947.

[4] R.J. Nemanich, S.A. Solin and G. Lucovsky, Solid St. Commun. **21** (1977) 273.

[5] W.J. Bresser, P. Boolchand, P. Suranyi and J.P. de-Neufville, Phys. Rev. Lett. **46** (1981) 1689.

[6] R.J. Nemanich, G.A.N. Connell, T.M. Hays and R.A. Street, Phys. Rev. **B18** (1978) 6900.

[7] P.M. Bridenbaugh, G.P. Espinosa, J.E. Griffiths, J.C. Phillips and J.P. Remeika, Phys. Rev. **B20** (1979) 4140.

[8] J.E. Griffiths, G.P. Espinosa, J.P. Remeika and J.C. Phillips, Phys. Rev. **B25** (1982) 1272.

[9] P. Boolchand, J. Grothaus, W.J. Bresser and P. Suranyi, Phys. Rev. **B25** (1982) 2975.

10] A. Fischer-Colbrie and P.H. Fuoss, J. Non-Cryst. Solids **126** (1990) 1.

[11] W. Pollard, J. Non-Cryst. Solids **144** (1992) 70.

[12] J.C. Phillips, J. Non-Cryst. Solids **43** (1981) 37.

[13] S. Susman, D.L. Price, K.J. Volin, R.J. Dejus and D.G. Montague, J. Non-Cryst. Solids **106** (1988) 26.

[14] G.D. Mahan, *Electron and Ion Spectroscopy of Solids* (Nato Advanced Study Institute series B32) eds. L. Fierman, J. Vennik and W. Dekeyser (Plenum Press, New York, London, 1978).

[15] C. Kittel, *Introduction to Solid State Physics* (Wiley, New York, 1986).

[16] V.K. Srivastava, Phys. Rev. **B29** (1984a) 6993; Phys. Lett. **102A** (1984b) 127; J. Phys. **C19** (1986) 5689; Phys. Rev. **B36** (1987) 5044.

[17] L.W. Martin, L.E. McNeil and J.M. Mikrut, Phil. Mag. **61** (1990) 957.

[18] M. Stevens, P. Boolchand and J.G. Hernandez, Phys. Rev. **B31** (1985) 981.

[19] L. Pauling, *The Nature of the Chemical Bond* (Ithaca, Cornell University, 1960) p.85.

[20] B.R. Orton, G. Saffarini, J. Gorgol and J.C. Riviere, Phil. Mag. **62** (1990) 71.

[21] G. Saffarini, X-ray photoelectron spectroscopy (XPS), X-ray diffraction (XRD), differential scanning calorimetry (DSC) and density study of ternary chalcogenide glasses based on $Ge-Se$ and $Ge-S$, Ph.D Thesis, Brunel University (1991).

[22] K. Tanaka, J. Non–Cryst. Solids **97** & **98** (1987) 391; J. Non–Cryst. Solids **103** (1988) 149; Phys. Rev. **B39** (1989) 1270.

TABLE CAPTIONS

Table 1 Peak fit parameters for the FSDP in $Ge_{1-x}Sn_xSe_2$ glasses.

Table 2 Plasmon energies (in eV) (measured and calculated), measured densities, measured glass transition temperatures, calculated average energy gaps and calculated average coordination numbers for $Ge_{1-x}Sn_xSe_2$ glasses.

Table 1

Composition	Peak Position Å^{-1}(± 0.03)	FWHM Å^{-1}(± 0.03)	Coherence length (Å)	Ratio FSDP/second peak
$GeSe_2$	1.14	0.16	39	0.46
$Ge_{0.9}Sn_{0.1}Se_2$	1.00	0.22	29	0.42
$Ge_{0.8}Sn_{0.2}Se_2$	1.00	0.22	29	0.45
$Ge_{0.7}Sn_{0.3}Se_2$	1.03	0.38	17	0.32
$Ge_{0.6}Sn_{0.4}Se_2$	1.03	0.38	17	0.22
$Ge_{0.5}Sn_{0.5}Se_2$	1.05	0.38	17	0.32

Table 2

Composition	$\hbar\omega_p$(exp.) eV (± 0.3)	$\hbar\omega_p$(calc.) eV	Density gcm^{-3} (±1%)	$T_g(K)$ ±(0.2%)	E_g eV	$< m >$
$GeSe_2$	17.7	16.0	4.45	687	5.42	2.67
$Ge_{0.9}Sn_{0.1}Se_2$	17.5	15.8	4.39	662	5.32	2.67
$Ge_{0.8}Sn_{0.2}Se_2$	17.3	15.5	4.31	642	5.22	2.67
$Ge_{0.7}Sn_{0.3}Se_2$	17.5	14.7	3.94	622	5.32	2.67
$Ge_{0.6}Sn_{0.4}Se_2$	16.6	14.2	3.76	608	4.88	2.67
$Ge_{0.5}Sn_{0.5}Se_2$	16.6	13.8	3.63	592	4.88	2.67
$Ge_{0.4}Sn_{0.6}Se_2$	16.5	13.5	3.52	588	4.84	2.67

FIGURE CAPTIONS

Fig.1 Change in density with Sn content in $Ge_{1-x}Sn_xSe_2$ glasses.

Fig.2 Change in glass transition temperature with Sn content in $Ge_{1-x}Sn_xSe_2$ glasses.

Fig.3 X–ray interference functions for $Ge_{1-x}Sn_xSe_2$ glasses,
(a) $x = 0.1$, (b) $x = 0.2$, (c) $c = 0.3$, (d) $x = 0.4$, and (e) $x = 0.5$.

Fig.4 Selenium Auger peaks in $Ge_{0.7}Sn_{0.3}Se_2$ (full curve) and $Ge_{0.5}Sn_{0.5}Se_2$ (dashed curve) shifted so that $^1G_4$ peaks coincide.

Fig.5 Change in plasmon energy with Sn content in $Ge_{1-x}Sn_xSe_2$ glasses both for calculated values ♦ and those determined experimentally ⊡ from the $L_3M_{4,5}M_{4,5}$ Auger lines of selenium.

Fig.6 Change in calculated values of the average energy gaps ⊡ and measured optical energy gaps ♦ [17] with Sn content in $Ge_{1-x}Sn_xSe_2$ glasses. The values of the optical energy gaps were normalized to the value of the average energy gap of a–$GeSe_2$.

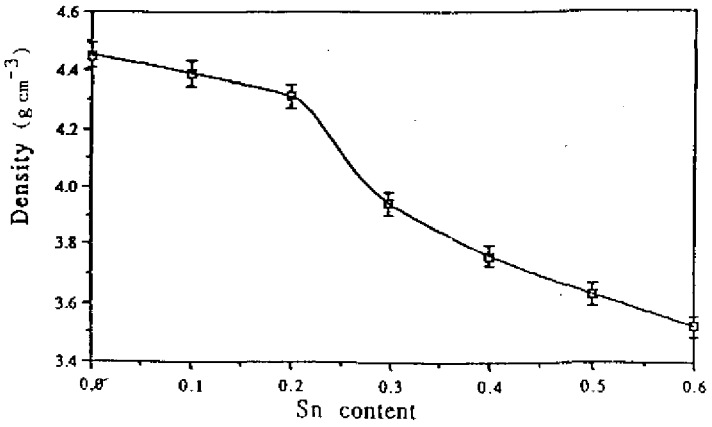

Fig.1

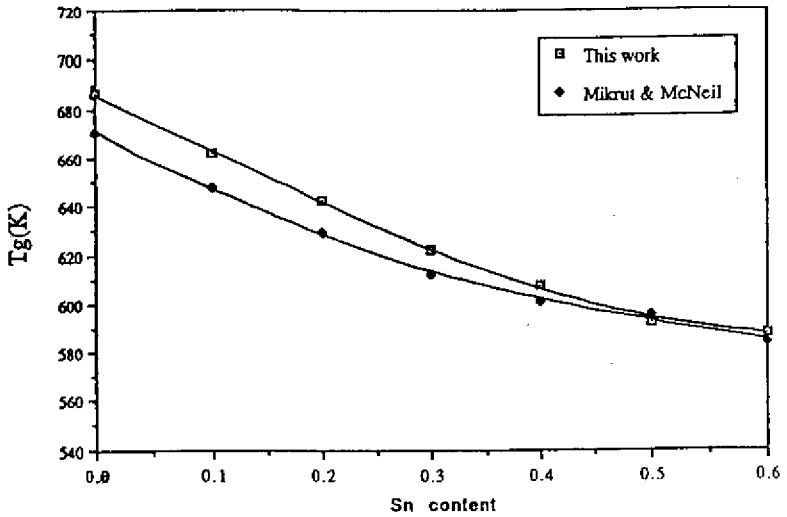
This work
Mikrut & McNeil
Tg(K)
Sn content
720
700
680
660
640
620
600
580
560
540
0.0
0.1
0.2
0.3
0.4
0.5
0.6

Fig.2

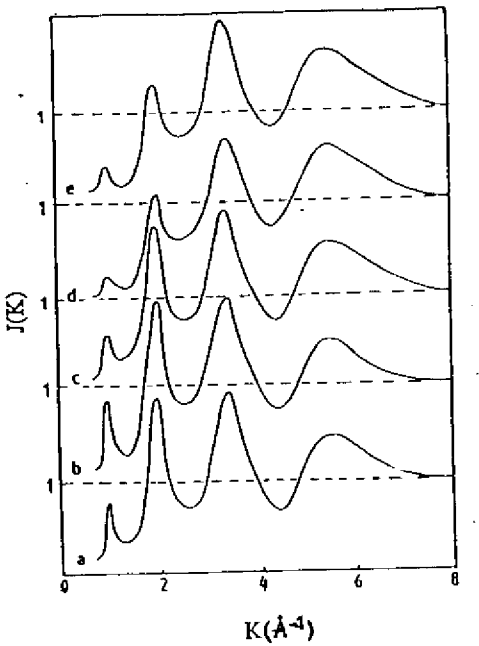
I(K)
K(Å⁻¹)
a
b
c
d
e
1
0
2
4
6
8

Fig.3

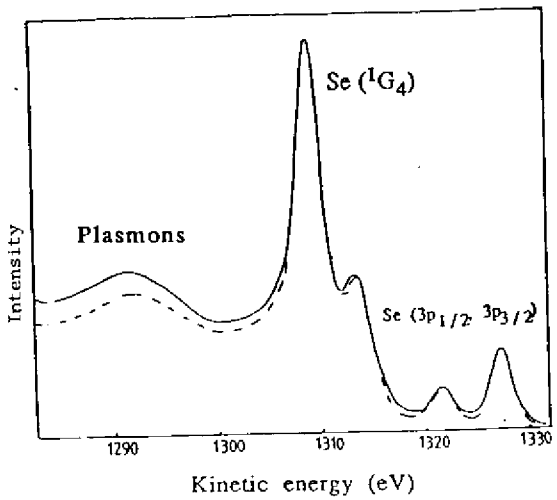
Se ($^1G_4$)
Plasmons
Se ($3p_{1/2}$, $3p_{3/2}$)
Intensity
1290
1300
1310
1320
1330
Kinetic energy (eV)

Fig.4

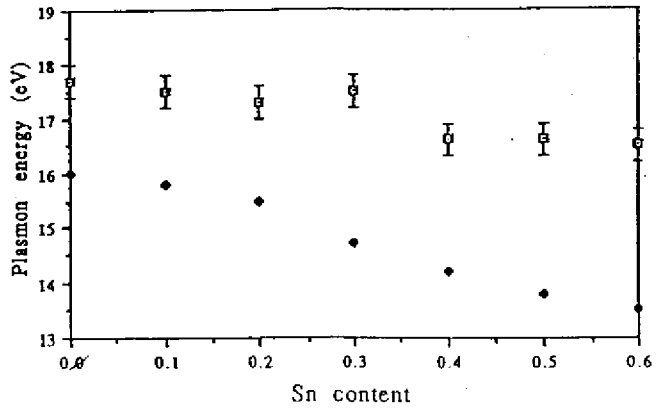
Plasmon energy (eV)
19
18
17
16
15
14
13
0.0
0.1
0.2
0.3
0.4
0.5
0.6
Sn content

Fig.5

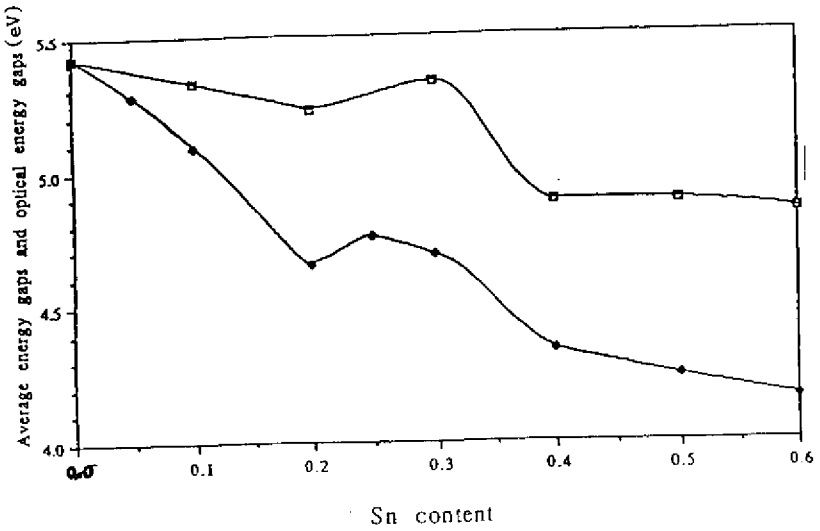
Average energy gaps and optical energy gaps (eV)
5.5
5.0
4.5
4.0
0.0
0.1
0.2
0.3
0.4
0.5
0.6
Sn content

Fig.6